Journal of
Mechanical
Science and
Technology

Journal of Mechanical Science and Technology 21 (2007) 2168~2177

A comparison of the effect of the electrohydrodynamic technique on the condensation heat transfer of HFC-134a inside smooth and micro-fin tubes

Suriyan Laohalertdecha and Somchai Wongwises*

Fluid Mechanics, Thermal Engineering and Multiphase Flow Research Lab. (FUTURE), Department of Mechanical Engineering, King Mongkut's University of Technology Thonburi, Bangmod, Bangkok 10140, Thailand

(Manuscript Received October 23, 2006; Revised June 13, 2007; Accepted June 18, 2007)

Abstract

The results of the condensation heat transfer enhancement and pressure drop of HFC-134a by using the electrohydrodynamic (EHD) technique are presented. The test section is a horizontal tube-in-tube heat exchanger where the refrigerant flows in the inner tube and water flows in the annulus. The outer tube is a smooth copper tube having outer diameter of 21.2 mm. Two types of inner tubes, smooth and micro-fin copper tubes, are tested. The outer diameter and length of both inner tubes is 9.52 mm and 2.5 m, respectively. A stainless steel cylindrical electrode of 1.47 mm in diameter is placed in the center of the tube. Experiments are conducted under conditions providing mass flux of 400 kg/m^{2}s, saturated temperature of 40 °C, heat flux of 20 kW/m^2 and applied voltage of 2.5 kV. The experimental results indicate that the EHD enhancements of the smooth tube are higher than those of the micro-fin tube over the range of average quality. The maximum heat transfer enhancements for smooth and micro-fin tubes are 1.1 times and 1.08 times, respectively. For a smooth tube, the pressure drop induced by EHD is considerably small. However, the application of EHD in a micro-fin tube can lead to 10 % increase in the pressure drop.

Keywords: Electrohydrodynamic; Condensation; Heat transfer enhancement; Smooth tube; Micro-fin tube

1. Introduction

Chlorofluorocarbons (CFCs), developed in the 1930s, are widely used as working fluids in many applications such as air conditioning and refrigeration because they are non toxic and non flammable. Unfortunately, chlorine molecules from CFCs destroy the ozone layer. HFCs consisting of carbon, hydrogen and fluorine are being used as alternatives to CFCs as they do not contain chlorine and are absolutely harmless to the ozone layer. Thus, HFCs can be used instead of CFCs because their thermo physical properties are very similar to those of CFCs. However, even though the difference in properties between both refrigerants is small, it may result in significant differences in the overall system performance. Therefore, the properties of HFCs should be studied in detail before they are applied.

The improvement in heat transfer performance of heat exchangers enables a considerable decrease in their size. In general, heat transfer enhancement techniques can be divided into two types: active and passive. This paper concentrates on the active techniques, especially the electrohydrodynamic (EHD) technique. The EHD technique is an active heat transfer enhancement technique that can induce secondary fluid motion which can enhance heat and mass transfer in single and two-phase flows. This interaction can result in the increase of fluid motion leading to a higher heat transfer coefficient. The general expression of EHD force is shown in Eq. (1).

*Corresponding author. Tel.: +662 470 9115, Fax.: +662 470 9111
E-mail address: somchai.won@kmutt.ac.th

$$f_e = qE - \frac{1}{2}E^2 \nabla\varepsilon + \frac{1}{2}\nabla\left\langle E^2\left(\frac{\partial\varepsilon}{\partial\rho}\right)_T \rho\right\rangle \quad (1)$$

The three terms on the right-hand side of Eq. (1) represent the Coulomb force, dielectrophoretic force, and electrostriction force, respectively. The Coulomb force is the only force that requires the presence of free charges in a fluid and is known as the electrophoretic force. The dielectrophoretic force is a consequence of inhomogeneity or spatial change in the permittivity of the dielectric fluid because of non-uniform electric fields, temperature gradients, and phase differences. The last term is the electrostriction force which occurs whether or not an applied field is uniform. This force depends on the non-uniformity of electric permittivity. A similar principle is applied when a charged needle electrode is brought close to a liquid surface. Fig. 1 shows the liquid surface extending into the gas toward the electrode and is called the liquid-extraction phenomenon. This again occurs due to the EHD-induced surface instability on the gas-liquid interface. The liquid-extraction phenomenon usually occurs in smooth tubes. Electro-convection is the phenomenon in which a previously quiescent fluid will start moving in a certain direction when a strong electric field is applied on the dielectric permittivity of the fluid as shown in Fig. 2. The electro-convection phenomenon usually occurs in micro-fin tubes.

The heat transfer enhancement using EHD technique has been studied by various researchers. Holmes and Chapman [1] experimentally investigated the effect of a non-uniform, alternating, 60-cycle, electric field on the condensation heat transfer of Freon-114. The condensing surface was a grounded cooled flat plate. A high voltage of 0-60 kV was supplied to a second plate placed above the first plate. The non-uniform electric field was controlled by changing the angle between both plates. The results indicated that at voltages less than 40 kV, reasonable agreement was obtained between the experimental data and predicted results. At high voltages over 40 kV, the results were unpredictable. The heat transfer coefficients in the presence of an electric field were approximately ten times higher than those without an electric field. Jia-Xiang et al. [2] investigated the EHD coupled heat transfer systems using a double electrode cylinder heat transfer model. The working fluid was Freon-11. The results indicated that the EHD had a significant effect on both boiling and condensation heat transfer. Singh et al. [3] investigated the effect of EHD on condensation heat transfer enhancement inside smooth and micro-fin tubes using HFC-134a as the working fluid. The test section consisted of a horizontal concentric tube in a tube heat exchanger with refrigerant flowing in the inner tube and water flowing in the annulus. Six different electrodes of various diameters and spacing were tested. The results showed that the EHD introduced an additional penalty of the pressure drop of 1200, 12.35 and 3.36 times higher than those without electrode for stratified flow, wavy flow and wavy annular flow, respectively. Cheung et al. [4] investigated the EHD-assisted external condensation on smooth horizontal and vertical tubes using HFC-134a as the working fluid. The effects of heat flux, electrode gaps and applied electric field potential were tested and discussed. It was found that the effective removal of the condensate through EHD-induced liquid extraction and dispersion phenomena was the mechanism of heat transfer augmentation. Silva et al. [5] studied the EHD enhancement of external condensation of pure HFC-134a on horizontal single enhanced tubes. Experiments were conducted on two types of commercial enhanced tubes at the high voltages of 0-25 kV, saturation temperatures of 10-40 °C, and heat fluxes of 10-40 kW/m^{2}K. The experimental results showed that the designed electrode worked well on the enhanced tubes, and was able to substantially improve the external condensation heat transfer coefficient.

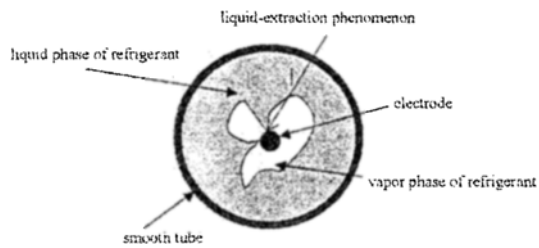

Fig. 1. Liquid-extraction phenomenon [3].

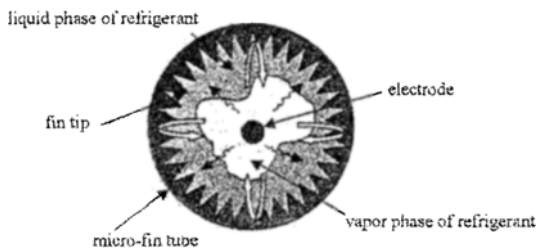

Fig. 2. Electro-convection phenomenon [3].

Table 1. Refrigerants and electrode-tube configurations investigated by various researchers.

Source	Refrigerant	Test condition	h_e/h_0 (maximum)	Note
Holmes and Chapman [1]	Freon-114	Voltage = 0-60 kV	Up to 10 times	External condensation
Jia-Xiang et al. [2]	Freon -11	Voltage = 0-15 kV	~1.85	External condensation Using double electrode
Singh et al. [3]	HFC-134a	Voltage = 0-sparkover kV $q = 8–22$ kW/m^2 $G = 50–300$ kg/m^2 s	6.5	Internal condensation Smooth and micro-fin tubes, $D_f = 12.7$ mm, L = 305 mm. Using Six different electrodes
Cheung et al. [4]	HFC-134a	Voltage = 0-26 kV $P_{sat} = 551.6$ kPa Electrode gap = 0.8,1.6,3.2 mm $q = 26-49$ kW/m^2	7.2	External condensation
Silva et al. [5]	HFC -134a	Voltage = 0-25 kV $q = 10-40$ kW/m^2 $T_{sat} = 10-40$ °C	~3	External condensation
Butrymowicz et al. [6]	HFC -123	Voltage = 22-25-27 kV	~2	External condensation
Laohalertdecha and Wongwises (2006)	HFC -134a	Voltage = 2.5 kV $q = 10-20$ kW/m^2 $T_{sat} = 40-60$ °C $G = 200–600$ kg/m^2 s	~1.1	Internal condensation Micro-fin tube, $D_f = 8.92$ mm, L = 2500 mm
Laohalertdecha and Wongwises (2007)	HFC -134a	Voltage = 2.5 kV $q = 10-20$ kW/m^2 $T_{sat} = 40-60$ °C $G = 200–600$ kg/m^2 s	~1.08	Internal condensation Smooth tube, $D_f = 7.9$ mm, L = 2500 mm

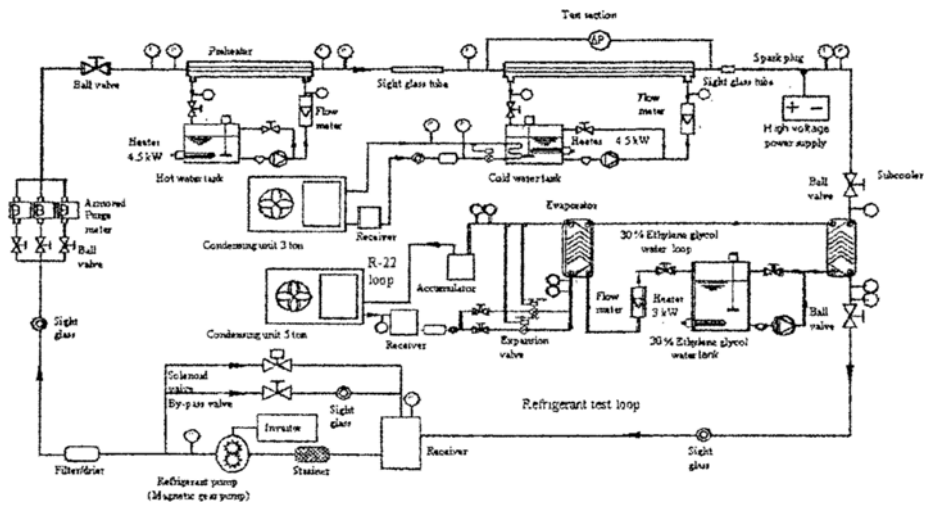

Fig. 3. Schematic diagram of experimental apparatus.

Butrymowicz et al. [6] presented a review on the passive and active enhancement of condensation heat transfer techniques concerning the augmentation of the condensate drainage. The method of condensate drainage enhancement by using a drainage strip was presented and a novel EHD technique was presented. For both methods, they provided their own experimental results and theoretical models. Laohalertdecha and Wongwises [7, 8] experimentally studied the effects of EHD on the condensation heat transfer and pressure drop of pure HFC-134a inside horizontal smooth and micro-fin tubes. The test section was a 2.5 m long concentric counter flow tube-in-tube heat exchanger with refrigerant flowing in the inner tube and cooling water flowing in the annulus. The inner tubes were made from smooth and micro-fin horizontal copper tubing of 9.52 mm outer diameter. The electrode was made from cylindrical stainless steel of 1.47 mm diameter. Some detailed information as described above is shown in Table 1.

It can be noted that almost all the experimental investigations found in literature are concerned with the

study of the EHD in a vessel or chamber; there are only few studies dealing with the application of EHD in a horizontal tube. In the present study, the objective is to study the effects of EHD on the heat transfer coefficient and pressure drop during condensation of HFC-134a flowing inside smooth and micro-fin tubes. Comparison of the pressure drop and heat transfer coefficient between the presence of the electrode and absence of the electrode is also discussed.

2. Experimental apparatus and method

The experimental apparatus compounds two sections including the refrigeration test and the DC high voltage power supply apparatus. The experimental apparatus was fabricated in order to determine the heat transfer coefficient and pressure drop of HFC-134a over the length of the test tube.

Fig. 3 shows the refrigerant loop that consists of a pre-heating loop, test section, cooling loop and chilling loop. The refrigerant is circulated by a gear pump controlled by an inverter. The refrigerant flows in series through a filter/dryer, a sight glass, a refrigerant flow meter, a pre-heater, a sight glass tube and enters the test section. The pre-heater controls the inlet quality before entering the test section. It is a spiral counter flow double tube heat exchanger designed to supply heat to prepare a controlled inlet quality for the vaporization of the refrigerant. After exiting the test section, the chilling loop condenses and sub-cools the refrigerant and removes the heat input from the pre-heater and test section and rejects the heat to the surroundings. Leaving the chilling loop, the refrigerant returns from two-phase refrigerant to a sub-cooled state. Eventually, the refrigerant returns to the refrigerant pump to complete the cycle.

A horizontal counter-flow tube-in-tube heat exchanger is fabricated as the test section. The length of the heat exchanger is 2.5 m. Fig. 4 shows the detailed dimensions of the heat exchanger and the location of the thermocouples. Fig. 5 shows the detailed cross-section of the micro-fin tube. Table 2 shows the dimensions of smooth and micro-fin tubes. A thermo-

Table 2. Dimensions of the test section.

Parameter	Micro-fin Tube	Smooth Tube
Outside diameter, D_o (m)	9.52×10^{-3}	9.52×10^{-3}
Bottom thickness, t (m)	0.3×10^{-3}	0.81×10^{-3}
Cross sectional area, A_c (m^2)	61.3×10^{-6}	49×10^{-6}
Wetted perimeter (m)	43.2×10^{-3}	24.81×10^{-3}
Maximum inside diameter, D_f (m)	8.92×10^{-3}	7.9×10^{-3}
Hydraulic diameter, D_h (m)	5.43×10^{-3}	7.9×10^{-3}
Fin pitch, p(m)	0.47×10^{-3}	-
Perimeter of one fin and channel taken perpendicular to the axis of the fin, S_p(m)	0.72×10^{-3}	-
Fin tip diameter, D_i(m)	8.52×10^{-3}	-
Bottom width, b_f(m)	0.27×10^{-3}	-
Fin height, e_f, (m)	0.2×10^{-3}	-
Apex angle, γ (degree)	52.45	-
Spiral angle, β (degree)	18	-
Number of fins, N	60	-

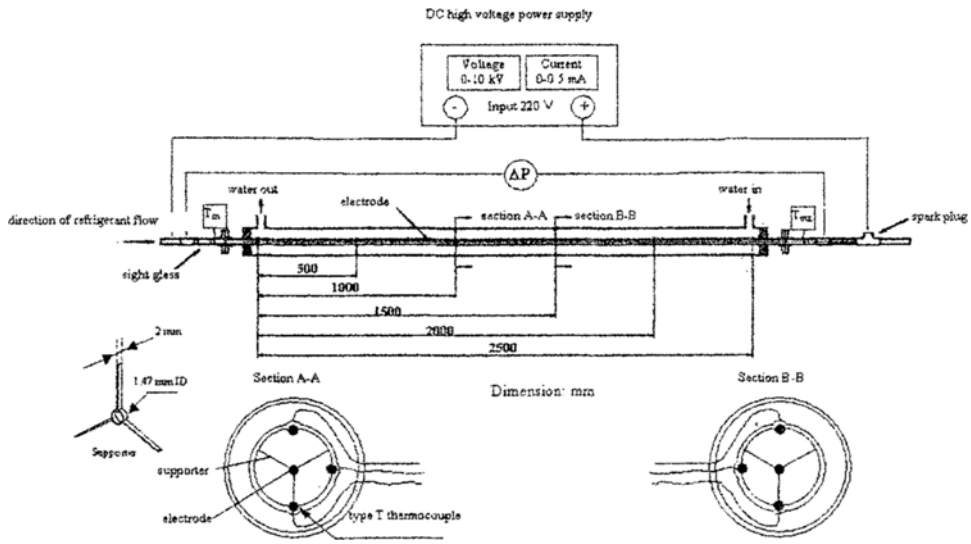

Fig. 4. Schematic diagram of the test section.

stat is used to control the inlet temperature of the water. Pressure drop is measured by a differential pressure transducer installed between the inlet and outlet of the test section. Temperatures across the test sec tion are measured by thermocouples. The length between pressure taps is 3 m. A low temperature thermostat is used to control the system pressure of the refrigerant flow.

Type-T thermocouples are used to measure refrigerant temperature and the tube wall temperatures in the test section. Fig. 4 shows a total of eighteen thermocouples located at the top, bottom and side at six points along the test tube. All the temperature measuring devices are well calibrated in a controlled temperature bath using standard precision mercury glass thermometers. The uncertainty of the temperature measurements is $\pm$ 0.1 °C. All static pressure taps are mounted on the tube wall. The refrigerant flow meter is a variable area type. The flow meter is specially calibrated in the range of 0–2.2 gal/min for HFC-134a by the manufacturer. The differential pressure transducer and pressure gauges are calibrated against a primary standard, the dead weight tester.

A stainless steel cylindrical wire, 1.47 mm in diameter, is used as electrode. The electrode is supported in the center of the test section by electrically insulating spacers (Teflon type material) at intervals of 250 mm. The electrode is attached to the spacers by using a special epoxy-resin. When the electric field is applied to the test section by a DC high voltage power supply, the electrode attached to a modified automotive spark plug serves as the charged electrode and the heat transfer surface as the receiving electrode, as shown in Fig. 4.

Fig. 6 shows a schematic diagram of the DC high voltage power supply. The electrical system design is a bridge rectifier circuit which contains 40 capacitors of 68μF (400 V each), a high voltage transformer, a variac transformer and other relevant instrumentation. The applied voltage of the power supply can be varied from 0 to 10 kV with a maximum current of 0.5 mA. The power supply is well calibrated against an electrostatic voltmeter.

Experiments were performed with mass flux of 400 kg/m^{2}s, heat flux of 20 kW/m^2, saturated temperature of 40 °C, various vapor qualities of refrigerant entering the test section, at the applied voltage of 2.5 kV. In the experiments, the refrigerant flow rate in the test section was controlled by adjusting the speed of the magnetic gear pump. To vary the average qualities of the test section, the heating water flow rate and the cooling water flow rate were varied by small increments while the refrigerant flow rate was kept constant. The cold water in the test section was circulated by centrifugal pump to remove heat from refrigerant

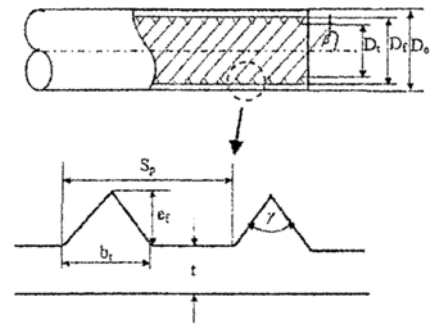

Fig. 5. Detailed cross section of micro-fin tube.

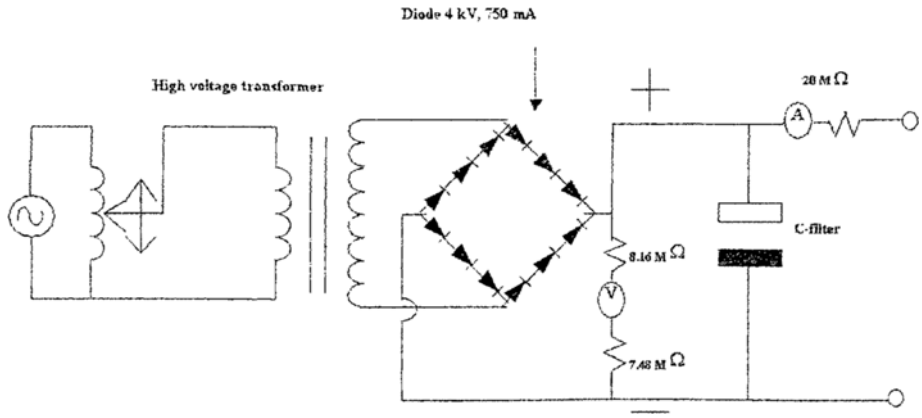

Fig. 6. Schematic diagram of DC high voltage power supply.

Table 3. Uncertainties of measured quantities and calculated parameters.

Parameter	Uncertainty
Temperature, T (°C)	± 0.1 °C
Pressure drop, ΔP (kPa)	± 0.37 kPa
Mass flow rate of refrigerant, m_{ref}	± 2 %
Mass flow rate of water, m_w	± 2 %
Heat transfer rate at test section, Q_{TS}	± 10 %
Heat transfer rate at pre-heater, Q_{ph}	± 5 %
Condensing heat transfer coefficient, h_{avg}	± 10 %
Average quality	± 5 %

to the water. During each experiment, the heat transferred from the test section was kept at a desired value.

This could be obtained by simultaneously adjusting and controlling the temperature and flow rate of the cold water entering the test section. The system was allowed to approach a steady state before any data was recorded. After the temperature, flow rate of refrigerant and heat flux at the measuring points were not fluctuating, a high voltage of 2.5 kV was applied to the test section. After stabilization, temperatures on the tube wall, temperature of refrigerant at the locations mentioned above, inlet and outlet temperatures of the heating water and cooling water and flow rates of heating water, cooling water and refrigerant were recorded. The pressure drop was measured by a pressure transducer installed between the inlet and outlet of the test section. The uncertainties of measured quantities and calculated parameters are shown in Table 3.

It is essential to realize that the maximum voltage before starting the electrical breakdown in the test section must be known and should not be exceeded during any steady-state condition performed in this study.

3. Data reduction

The data reduction of the measured results can be analyzed as follows:

3.1 The inlet vapor quality of the test section ($x_{TS,in}$)

$$x_{TS,in} = \frac{i_{TS,in} - i_{f@T_{TS,in}}}{i_{fg@T_{TS,in}}} \tag{2}$$

where $i_{f@T_{TS,in}}$ is the enthalpy of the saturated liquid based on the temperature of the test section inlet, $i_{fg@T_{TS,in}}$ is the enthalpy of vaporization based on the temperature of the test section inlet, $i_{TS,in}$ is the refrigerant enthalpy at the test section inlet and is given by

$$i_{TS,in} = i_{ph,in} + \frac{Q_{ph}}{m_{ref}} \tag{3}$$

where $i_{ph,in}$ is the inlet enthalpy of the liquid refrigerant before entering the pre-heater, m_{ref} is the mass flow rate of the refrigerant and Q_{ph} is the heat transfer rate in the pre-heater:

$$Q_{ph} = m_{w,ph} c_{p,w} (T_{w,in} - T_{w,out})_{ph} \tag{4}$$

where $m_{w,ph}$ is the mass flow rate of the water entering the preheater, $c_{p,w}$ is specific heat of water, $(T_{w,in} - T_{w,out})_{ph}$ is temperature difference between inlet and outlet position of the preheater.

3.2 The outlet vapor quality of the test section ($x_{TS,out}$)

$$x_{TS,out} = \frac{i_{TS,out} - i_{f@T_{TS,out}}}{i_{fg@T_{TS,out}}} \tag{5}$$

where $i_{TS,out}$ is the refrigerant enthalpy at the test section outlet, $i_{f@T_{TS,out}}$ is the enthalpy of the saturated liquid based on the temperature of the test section outlet, and $i_{fg@T_{TS,out}}$ is the enthalpy of vaporization. As a consequence, the outlet enthalpy of the refrigerant flow is calculated as

$$i_{TS,out} = i_{TS,in} - \frac{Q_{TS}}{m_{ref}} \tag{6}$$

The heat transfer rate in the test section is obtained from

$$Q_{TS} = m_{w,TS} c_{p,w} (T_{w,out} - T_{w,in})_{TS} \tag{7}$$

where $m_{w,TS}$ is the mass flow rate of the water entering the test section and $(T_{w,out} - T_{w,in})_{TS}$ is temperature difference between outlet and inlet position of the test section.

3.3 The average heat transfer coefficient

$$h_{avg} = \frac{Q_{TS}}{A_{inside} (T_{avg,sat} - T_{avg,wall})} \tag{8}$$

where h_{avg} is the average heat transfer coefficient, Q_{TS} is the heat transfer rate in the test section, $T_{avg,wall}$ is the average temperature of the wall, $T_{avg,sat}$ is the average temperature of the refrigerant at the test section inlet and outlet and A_{inside} is the inside surface area of the test section:

$$A_{inside} = \pi D_f L \tag{9}$$

D_f is the inside diameter of the test tube. L is the length of the test tube. The inside diameter of the micro-fin tube is defined as the outer diameter of the micro-fin tube minus twice the minimum wall thickness.

4. Results and discussion

The results of condensation heat transfer enhancement and pressure drop of HFC-134a by using the electrohydrodynamic (EHD) technique are presented. The experimental test runs have been selected to cover the broadest range of average quality experimentally possible. The test conditions are set average saturated temperature of 40 °C, mass flux of 400 kg/m^{2}s, heat flux of 20 kW/m^2 and applied voltage of 2.5 kV. The results obtained by Nualboonrueng et al. [9] correspond to the absence of an electrode and are compared with those in this study with the presence of an uncharged electrode and a charged electrode in the smooth and micro-fin tubes.

4.1 Heat transfer coefficient

Fig. 7 shows a comparison of the average heat transfer coefficients results obtained from various installations including the absence of an electrode, the presence of an uncharged electrode (0 kV) and the presence of a charged electrode (2.5 kV) in the smooth tube at a saturation temperature of 40 °C, mass flux of 400 kg/m^{2}s, and heat flux of 20 kW/m^2.The average quality is calculated as the arithmetic mean between the inlet and outlet qualities of the test section. During condensation, the liquid film thickness gradually increases. The thermal resistance is therefore increased resulting in a decrease in the heat transfer rate. The experimental results show that higher average quality increases the average heat transfer coefficient because a higher vapor velocity produces higher shear stress at the vapor-liquid interface. This increasing shear stress causes more waves

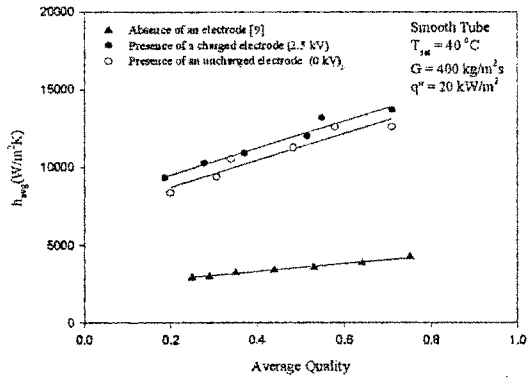

Fig. 7. Condensation heat transfer coefficient versus average quality for smooth tube.

on the surface of the liquid film and, as a result, increases the surface area for heat transfer. Therefore, the result is that the average heat transfer coefficient increases with increasing average quality. The average heat transfer coefficient obtained with presence of an uncharged electrode is approximately higher 3-5 times than with the absence of electrode at the same average quality. This is because the supporter and electrode promote turbulent flow, leading to better convection heat transfer. The maximum heat transfer enhancement is about 1.1 times.

The average heat transfer coefficient obtained with the presence of a charged electrode is higher than that with an uncharged electrode at the same average quality because of the instabilities at the liquid-vapor interface resulting from the molecules of refrigerant disturbed by the EHD force; this phenomenon is called "liquid-extraction". The refrigerant vapor phase having low dielectric permittivity is pushed by the EHD force to the inside tube surface. On the other hand, the liquid phase of refrigerant having high dielectric permittivity is moved from the inside tube surface towards the electrode surface. The condensate film thickness at the inside tube wall is reduced by liquid-extraction, promoting secondary fluid motion inside the liquid film. At higher average quality, the difference between a heat transfer coefficient with the presence of a charged electrode and that with an uncharged electrode is reduced. This is because higher axial momentum resulting from higher vapor velocity dominates the EHD force. However, the EHD force is high enough for increasing heat transfer coefficient at all average qualities.

Fig. 8 shows a comparison of the average heat transfer coefficients results obtained from various

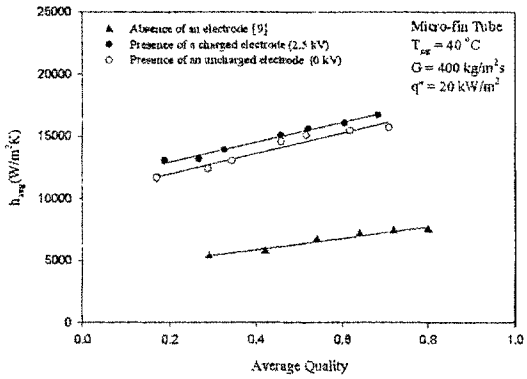

Fig. 8. Condensation heat transfer coefficient versus average quality for micro-fin tube.

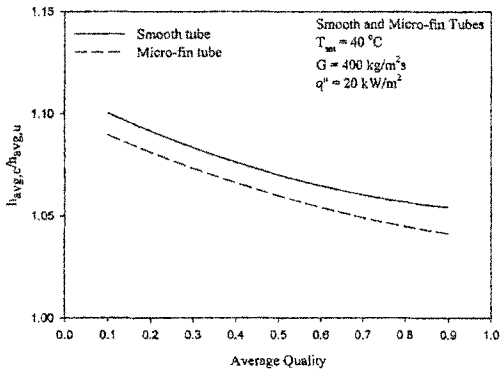

Fig. 9. EHD heat transfer enhancement ratio versus inlet quality for smooth and micro-fin tube.

installations including the absence of an electrode, the presence of an uncharged electrode (0 kV) and the presence of a charged electrode (2.5 kV) in the micro-fin tube at a saturation temperature of 40 °C, mass flux of 400 kg/m^{2}s, and heat flux of 20 kW/m^2. This figure also shows that the average condensation heat transfer coefficient for the presence of a charged electrode and the presence of an uncharged electrode increases with increasing average quality. This is because of a reduction of thermal conduction resistance in the liquid layer caused by thinning of the liquid layer. In addition, the average condensation heat transfer coefficient with the presence of a charged electrode is higher than that with an uncharged electrode. This is due to the ion-induced electro-convection phenomenon in which a strong electric field polarizes the dielectric liquid that is therefore moved radially to the electrode surface having maximum electric field strength. The average heat transfer coefficient obtained with presence of an uncharged electrode is approximately 2.5-3 times higher than with the absence of electrode at the same average quality. This is because the supporter and presence of electrode can induce turbulent flow, which is an important mechanism in convective heat transfer. The maximum heat transfer enhancement is about 1.08 times.

Fig. 9 shows the condensation heat transfer enhancement ratio with average quality of pure HFC-134a in smooth and micro-fin tubes at a saturation temperature of 40 °C, heat flux of 20 kW/m^2, mass flux of 400 kg/m^{2}s and voltage of 2.5 kV. The heat transfer enhancement ratio is defined by $h_{avg,c}/h_{avg,u}$ where $h_{avg,c}$ is the heat transfer coefficient with the presence of a charged electrode and $h_{avg,u}$ is the heat transfer coefficient with the presence of an uncharged electrode. The heat transfer enhancement ratio is determined from the measured data in Figs. 7 and 8. The heat transfer enhancement ratios of the smooth tube are higher than those of the micro-fin tube across the range of the average quality as shown in Fig. 9. This is because smooth and micro-fin tubes do not possess the same heat transfer surface. Therefore, electric field distributions of smooth and micro-fin tubes are different. When the smooth tube is applied with the coaxial cylindrical electrode, the highest electric field is at the electrode surface because of its small radius of curvature. In this case, the heat transfer enhancement from using the EHD technique is expected to be high due to the instabilities at the liquid-vapor interface resulting from the molecules of refrigerant disturbed by the EHD force. This is the so-called liquid-extraction phenomenon as shown in Fig 1. The vapor phase of refrigerant having low dielectric permittivity is pushed by the EHD force to the inside tube surface. On the contrary, the liquid phase of refrigerant having high dielectric permittivity is therefore pulled from the inside tube surface toward the electrode surface. This phenomenon promotes secondary fluid motion inside the liquid film and leads to the reducing of condensate film thickness at the inside tube wall. When a coaxial cylindrical electrode is used with a micro-fin tube, the highest electric field is at the tip of the fin due to its small radius of curvature (sharp) since the liquid interface is pulled toward the tip of the fin, as shown in Fig. 2. In this case, the heat transfer enhancement using the EHD technique is not expected to be high. However, in this case, liquid extraction is greatly suppressed and the only enhancement obtained is due to electro-convection. Electro-convection is a phenomenon in which, when a strong

electric field is applied on the dielectric permittivity of a fluid which is previously quiescent, the fluid will start moving in a certain direction, as shown in Fig. 2.

4.2 Pressure drop

The advantage of the EHD technique is the enhancement of the heat transfer. However, this must always be considered together with the associated change in pressure drop. The following paragraphs present the measured pressure drops during condensation of HFC-134a at high mass flux with the absence of an electrode, the presence of an uncharged electrode and the presence of a charged electrode over a range of experimental conditions in horizontal smooth and micro-fin tubes.

The variation of the measured pressure drop with average quality of pure HFC-134a during condensation in smooth and micro-fin tubes at a saturation temperature of 40 °C, heat flux of 20 kW/m^2 and mass flux of 400 kg/m^2 s is shown in Figs. 10 and 11. The pressure drop shown in these figures is obtained by dividing the measured pressure drop by the length between pressure taps. In the apparatus used in this study, the length between pressure taps is 3 m while the length of the heat exchanger is 2.5 m. The experimental test runs are selected to cover the broadest range of average quality. These figures show that the measured pressure drops obtained from the presence of an uncharged electrode in the flow field increase approximately 5 times because the supporter and electrode obstruct the flow field. The pressure drop with the absence of an electrode, the presence of an uncharged electrode, the presence of a charged electrode increases with increasing average quality.

For both smooth and micro fin tubes, the pressure drop with the presence of a charged electrode is higher than that with an uncharged electrode across the range of the average quality. This is because the EHD applied on the flow field promotes turbulent flow, leading to higher pressure drop. In addition the experimental results also show that the difference of pressure drop between the presence of a charged electrode and an uncharged electrode in micro fin tubes is more significant than that in smooth tubes. Since the area having highest electric field in the micro-fin (at the fin tip) is larger than that in the smooth tube (at the electrode surface), perturbations and waviness in the condensate film in micro-fin tube obtained from electro-convection phenomenon are much higher than

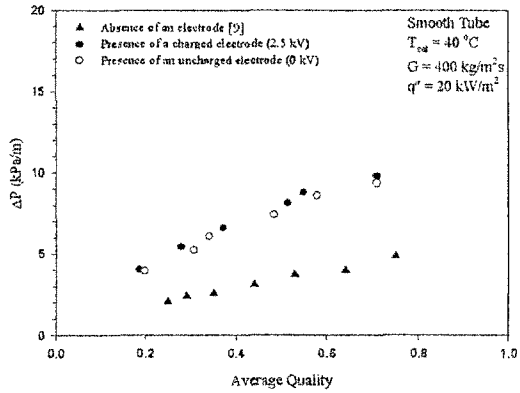

Fig. 10. Pressure drop versus average quality for smooth tube.

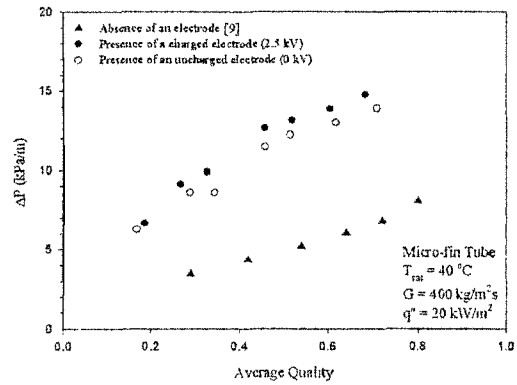

Fig. 11. Pressure drop versus average quality for micro-fin tube.

those in the smooth tube obtained from the liquid-extraction phenomenon. This causes the pressure drop to increase.

5. Conclusion

The present paper reports the effect of the electrohydrodynamic force on condensation heat transfer enhancement of HFC-134a in horizontal smooth and micro-fin tubes with cylindrical electrode. The presence of an uncharged electrode (0 kV) in the flow field contributes to improve the heat transfer coefficient and pressure drop by 3-5 times because the supporter enhances the flow turbulence, which leads to even better convection heat transfer. The maximum enhancement by EHD for average heat transfer coefficient in smooth and micro-fin tubes is 1.1 times and 1.08 times, respectively. The pressure drop obtained from the application of an EHD voltage of 2.5 kV in micro-fin tubes is higher than that in smooth tubes across the range of average quality.

Acknowledgments

The present study was supported financially by the Joint Graduate School of Energy and Environment (JGSEE) and the Thailand Research Fund (TRF) whose guidance and assistance are gratefully acknowledged.

Nomenclature

A_{inside} : Inside surface area of the test section (m^2)
A_c : Cross-section area (m^2)
b_t : Bottom width (m)
c_p : Specific heat at constant pressure (J/kg K)
D_h : Hydraulic diameter (m)
D_f : Maximum inside diameter of the test section(m)
D_o : Outside diameter (m)
D_t : Fin tip diameter (m)
E : Electric field strength (V/m)
e_f : Fin height (m)
f_e : Unit force density (N/m^3)
G : Mass flux (kg/m^2 s)
h : Heat transfer coefficient (W/m^2 K)
i : Enthalpy (J/kg)
L : Length of the test tube (m)
m : Mass flow rate (kg/s)
N : Number of fins
P : Pressure (kPa)
ΔP : Pressure drop (kPa/m)
Q : Heat transfer rate (W)
S_p : Perimeter of one fin and channel taken perpendicular to the axis of the fin (m)
q : Electric charge density (C/m^3)
q" : Heat flux (W/m^2)
T : Temperature (°C)
t : Bottom thickness (m)
x : Quality

Greek letters

β : Spiral angle (degree)
γ : Apex angle (degree)
ρ : Condensate density (kg/m^3)
ε : Electric permittivity (F/m)

Subscripts

avg : Average
c : Charged electrode
f : Saturated liquid
fg : Difference in property between saturated liquid and vapor
in : Inlet
u : Uncharged electrode
out : Outlet
ph : Pre-heater
ref : Refrigerant
sat : Saturation
TS : Test section
w : Water

References

[1] R. E. Holmes and A. J. Chapman, Condensation of Freon-114 in the presence of a strong nonuniform alternating electric field, *Journal of heat transfer, Transaction of ASME*. (1970) 616-620.

[2] Y. Jia-Xiang, D. Li-Jian and H. Yang, An experimental study of EHD coupled heat transfer, IEEE Conference on Electrical Insulation and Dielectric Phenomena, San Francisco, USA. (1996).

[3] A. Singh, M. M. Ohadi and S. Dessiatoun, EHD enhancement of in-tube condensation heat transfer of alternate refrigerant R-134a in smooth and microfin tubes, ASHRAE Transactions: Symposia. (1997) 813-823.

[4] K. Cheung, M. M. Ohadi and S. V. Dessiatoun, EHD-assisted external condensation of R-134a on smooth horizontal and vertical tubes, *International Journal of Heat and Mass Transfer*. 42 (1999) 1747-1755.

[5] L. W. D. Silva, M. Molki and M. M. Ohadi, Electrohydrodynamic enhancement of R-134a condensation on enhanced tubes, IEEE Industry Applications Conference, Rome, Italy. (2000).

[6] D. Butrymowicz, T. Marian and J. Karwacki, Enhancement of condensation heat transfer by means of passive and active condensate drainage techniques, *International Journal of Thermal Science*. 26 (2002) 473-484.

[7] S. Laohalertdecha and S. Wongwises, Effects of electrohydrodynamic on heat transfer coefficient and pressure drop during condensation of HFC-134a flowing inside micro-fin horizontal tubes, *Experimental thermal and Fluid Science*. 30 (2006) 675-686.

[8] S. Laohalertdecha and S. Wongwises, Effect of EHD on heat transfer enhancement during two-phase condensation of R-134a at high mass flux in a horizontal smooth tube, *Heat and Mass Transfer*. 43 (2007) 871-880.

[9] T. Nualbobnrueng, J. Kaewon and S. Wongwises, Two-phase condensation heat transfer coefficient of HFC-134a at high mass flux in smooth and microfin tubes, *International Communications in Heat Mass Transfer*. 30 (2003) 577-590.